Scaling Analysis of the Sea Surface Temperature Anomaly in the South China Sea

ZIJUN GAN

LED, South China Sea Institute of Oceanology, Chinese Academy of Sciences, Guangzhou, China

YOUFANG YAN

LED, South China Sea Institute of Oceanology, Chinese Academy of Sciences, Guangzhou, and Graduate School of the Chinese Academy of Sciences, Beijing, China

YIQUAN QI

LED, South China Sea Institute of Oceanology, Chinese Academy of Sciences, Guangzhou, China

(Manuscript received 20 September 2005, in final form 22 February 2006)

ABSTRACT

Based on the data of optimum interpolation sea surface temperature (OISST), the temporal correlations of the sea surface temperature anomaly (SSTA) in the South China Sea (SCS) are studied by using the rescaled range analysis (R/S) and detrended fluctuation analysis (DFA). The results show that the scaling exponents of SSTAs are larger than 0.8. This finding indicates that the SSTAs in the SCS exhibit persistent long-range time correlation of the fluctuations and the interval spreads over a wide period, from about 1 month to 4.5 yr (4~235 weeks). In addition, the "degree" of the correlations depends very much on the geographic locations: near to the coastal regions, the value is small, while far from the coastline, the value is relatively larger. This means that SSTAs in the central SCS are smoother than those of the coastal regions. The persistence of SST in the SCS may be used as a "minimum skill" to assess the ocean models and to evaluate their performance.

1. Introduction

Global climate change and its local response is a leading issue for oceanographers and climatologists in the twenty-first century. To understand the processes involved in global climate change, many different scientific measurements are needed. One of the critical parameters for understanding how the ocean is connected with climate on a global scale is the sea surface temperature (SST). Although SST can be measured, it is not always easy to analyze because it may exhibit irregular and nonlinear evolution that varies with the temporal and spatial scale. To characterize the SST variability on all pertinent temporal and spatial scales still poses a challenge to academic researchers.

Recently, there is an increasing emphasis on analyzing the time series from the viewpoint of complexity. Long-range persistence or dependence, as one of the characteristics of evolutionary complex system, has been studied in many fields (Peng et al. 1994; Liu et al. 1997; Havlin et al. 1999; Matsoukas et al. 2000).

The South China Sea (SCS) is a semiclosed ocean basin (see Fig. 1), connected to the surrounding oceans via straits. It has unique characteristics compared to the open ocean and the land surface. As a part of warm pool in the western Pacific Ocean and a primary thermal resource of heat to the atmosphere through frequent convection, the SCS strongly impacts the rainfall of Yangtze River, the Huaihe River basin, and southern Japan. It is also tied to other important climate phenomena, such as typhoons and ENSO. Various studies have focused on SST and its variability in the SCS (Wang et al. 1996; Chu et al. 1997; Ose et al. 1997; Tian et al. 2000; Qu 2001). However, few have approached the problem from the viewpoint of an evolutionary complex. In this paper, we take this view and apply the scaling analysis methods to investigate the long-range-

Corresponding author address: Dr. Youfang Yan, South China Sea Institute of Oceanology, Chinese Academy of Sciences, 164 W. Road, Xingang, 510301 Guangzhou, China.
E-mail: youfangyan@scsio.ac.cn

DOI: 10.1175/JTECH1981.1

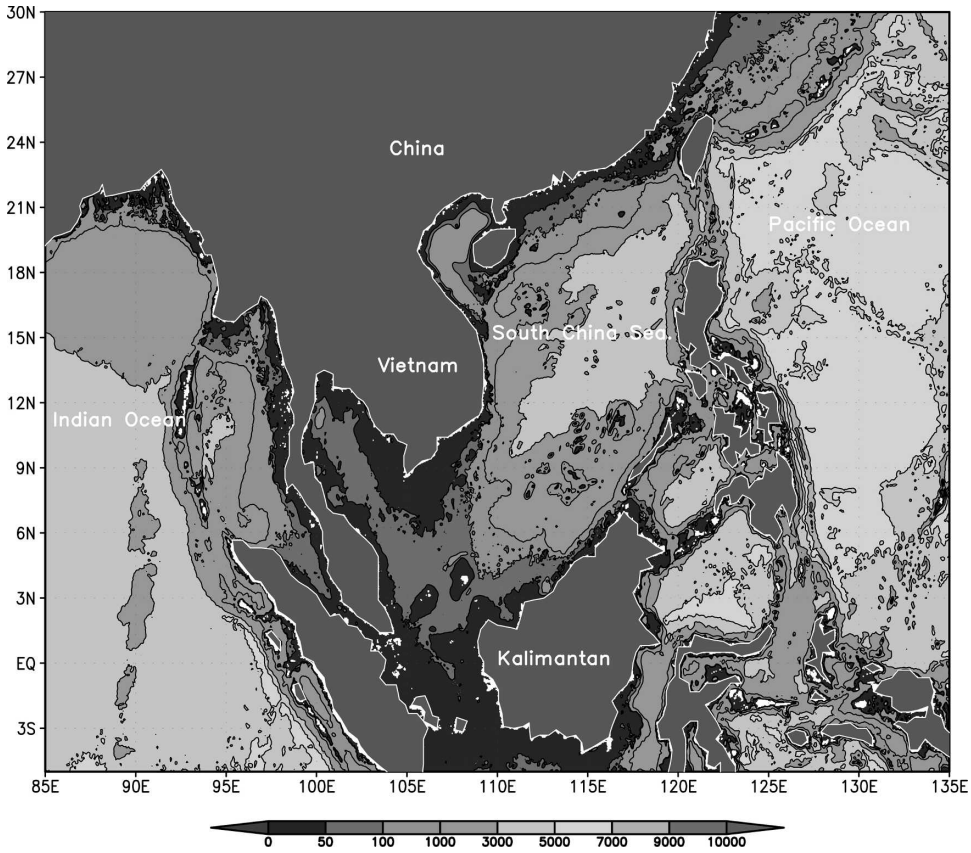

FIG. 1. Map of the South China Sea and its adjacent regions with isobaths showing the bottom topography. Contours schematic (m) with interval of 0, 50, 100, 1000, 3000, 5000, 7000, 9000, and 10 000.

dependent characteristics of the sea surface temperature anomaly (SSTA) and hope it may be served as a nontrivial test bed for the ocean models and allow for evaluation of their performance in the SCS.

The paper is organized as follows. In section 2, the data are introduced briefly. In section 3, a short review of scaling analysis methods is presented to make the paper more self-contained. In section 4, we present the results and discussions, and the conclusions are drawn in section 5.

2. Study area and data used

The study area is located between 0.5°–24.5°N latitude and 99.5°–124.5°E longitude and the corresponding data are taken from the weekly optimum interpolation sea surface temperature (OISST) with a spatial resolution of 1° × 1° from 1982 to 2003 (Reynolds and Smith 1994).

The annual cycle of SST is obvious. To remove the period perturbations, we focus our study on the anomaly time series of SST, namely, SST $A(k, n) = \mathrm{SST}(k, n) - \langle \mathrm{SST}(k) \rangle$, where $\langle \mathrm{SST}(k) \rangle = (1/22)\Sigma_{n=1982}^{2003}\mathrm{SST}(k, n)$ is the mean SST in the kth week over all years (1982–2003, with a total of 22 yr), $k = 1, 2, 3, \ldots$, is the calendar week, and $n = 1982, \ldots, 2003$ is the calendar year (see Fig. 2).

3. Methods used

The analysis of a given temporal sequence with apparently random fluctuation was begun by asking whether the value of the signal at a given instant had any correlation with the value at a later time. The standard statistical method for describing the signal is the temporal correlation. The corresponding Fourier transform of the correlation function is the spectral density. For a complex system comprised of various interacting subsystems, the correlation function is very different from that of a simple system, which has exponential decay with time. In a complex system, the correlation may decay with a power-law form (Sprott 2003)

$$C(\tau) \sim \tau^{-\gamma}, 0 < \gamma < 1, \quad (1)$$

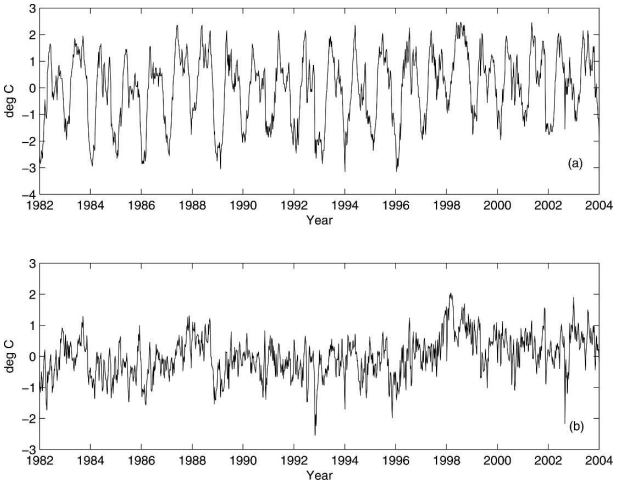

FIG. 2. (a) The fluctuation of SST in the central SCS (14.5°N, 112.5°E) and (b) the corresponding SSTA in the central SCS.

where $C(\tau)$ is an autocorrelation function, τ is the lag, γ is the autocorrelation exponent and "$\sim$" means asymptotic equivalence. Equation (1) implies that the system exhibits long-range correlated (persistent or dependent) behavior. For a long-range correlated process, the power spectral function $S(f)$ can be written as

$$S(f) \sim f^{-\beta}, 0 < \beta < 2, \tag{2}$$

where f is the frequency and β is the spectral density scaling exponent. Additionally, Eq. (2) is called the "1/*f*-like noise" spectrum, which implies that the current value of the signal varies not only with its most recent value but also with its long-term history in a scale-invariant, fractal manner (Bak 1996).

The idea of scale invariance is that if a sequence $x(t)$ fulfills the following expression:

$$x(t) \overset{\text{def}}{=\!=} a^{-H}x(at), a > 0, \tag{3}$$

then the sequence is scale invariant or self-affine. Here the symbol "def" denotes that the sequence $x(at)$ and $x(t)$ have identical distribution. Self-affinity indicates that the graph $x(t)$ remains statistically unchanged when the time axis and the amplitude are scaled by a factor a and a^{-H}, respectively. The Hurst exponent H quantifies the degree of long-range dependence as well as the asymptotic self-affine scaling of a sequence with $0 < H < 1$. Self-affinity is also called self-similarity when the sequence is isotropic (i.e., $H = 1$).

To quantitatively characterize a long-range correlated process is not easy because it inseparably involves both stationarity and nonstationarity. Thus, in this work the conventional methods such as the autocorrelation function and power spectral analysis do not satisfy our demands to quantify the long-range dependence.

A nonlinear approach, that is, rescaled range analysis (R/S), is applied (Hurst 1951). Considering a discrete time series $x(t)$ ($t = 1, 2, \ldots, T$), let $y(t, \tau) = \Sigma_{i=1}^{t}[x(i) - \langle x(\tau)\rangle], i = 1, 2, \ldots, t \le \tau \le T$ be the cumulative deviation from the mean $\langle x(\tau)\rangle$; the range of the difference between the maximum and the minimum values of $y(t, \tau)$ is given as

$$R(\tau) = \max[y(t, \tau)] - \min[y(t, \tau)]. \tag{4}$$

Let $S(\tau)$ be the standard deviation of $x(t)$ in the period of τ; the rescaled range $R(\tau)/S(\tau)$ is a dimensionless variable with scales τ as follows:

$$\langle R(\tau)/S(\tau)\rangle \sim \tau^{H}, \tag{5}$$

where the angle brackets $\langle\rangle$ denote the average of $R(\tau)/S(\tau)$ and H is the Hurst exponent, which provides a quantitative measurement of the strength of persistence and antipersistence for a time series with $0 < H < 1$. When $H = 1$, the time series has a perfect correlation between increments. If $0.5 < H < 1$, the time series has persistence (positive correlation), meaning that a large value is more likely to be followed by a large value. When $H = 0.5$, the series is random, and when $0 < H < 0.5$ the time series is antipersistent (negative correlation). As an early method of studying the natural fractal geometry, R/S can a distinguish random time series from a correlated one and provide a measure of a sequence roughness (Feder 1988; Peters et al. 2002; Sprott 2003), but it also has many disadvantages and limitations because it relies on the maximum and the minimum values of the sequence (North and Halliwell 1994).

A novel method, detrended fluctuation analysis (DFA) method, is more effective and robust to determine fractal scaling properties and long-range dependence in noisy, nonstationary time series (Peng et al. 1994, 1995). To implement the DFA method, the integrated time series $y(k)$ of the original time series $x(i)$ (total length N) is written as

$$y(k) = \sum_{i=1}^{k}[x(i) - \langle x\rangle], \tag{6}$$

where $\langle x\rangle$ is the average of the time series, and it splits the original $y(k)$ time series into $l \equiv \text{int}(N/n)$ nonoverlapping segments with equal length n. After the integrated time series is deviated into j segments, a polynomial $y_n^{(p)}(k)$ of p order is fitted to the time series to obtain the local trend in the particular segment. We define the detrended time series for segment duration n as $y_n^{(p)}(k)$. For a given box size n, the characteristic size of fluctuation for this integrated and detrended time series is then calculated by

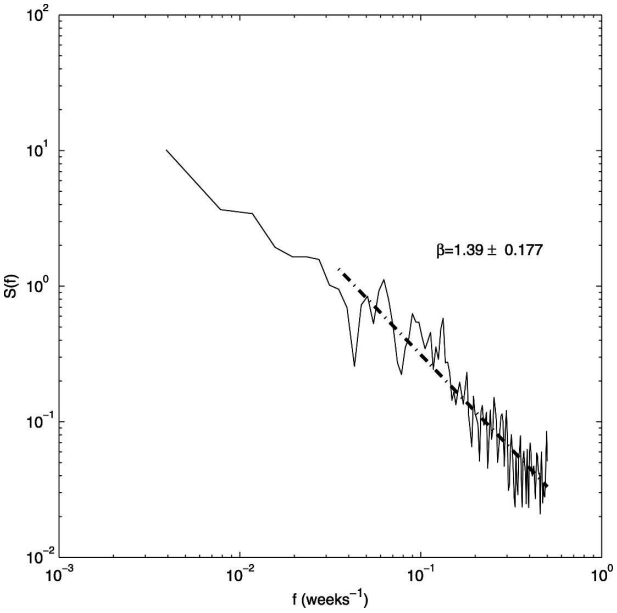

FIG. 3. The power spectrum analysis of SSTA in the central SCS (14.5°N, 112.5°E). The scaling exponents estimation is given by the slope with exponent $\beta \approx 1.39 \pm 0.177$.

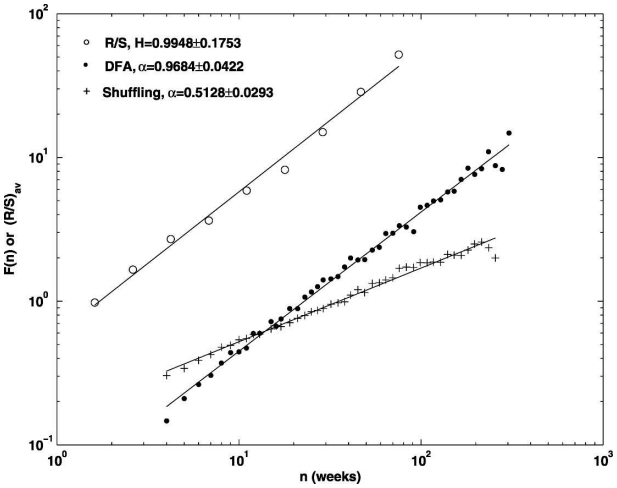

FIG. 4. The R/S analysis and DFA analysis ($4 \le n \le N/4$) on SSTA in the central region (14.5°N, 112.5°E). The scaling exponents estimation given by a least squares linear fitting of the slope show that the SSTA exhibits long-range-dependent behavior. To test whether the long-range-dependent behavior really does exist, the shuffle analysis method is performed to shuffle the origin series randomly without changing its statistical parameter, then do the DFA analysis again. The exponent of shuffling data ($\alpha \approx 0.50$) proves further that the original SSTA is long-range dependent.

$$F(n) = \sqrt{\frac{1}{N^*}\sum_{k=1}^{N^*}[y(k) - y_n^{(p)}(k)]^2}, \qquad (7)$$

where $N^* = ln$, $p = 1$. The reason we only use order $p = 1$ is because higher orders do not reveal any further structure in the time series (Kiraly and Janosi 2002). This computation is repeated over all time scales (box sizes) to provide a relationship between $F(n)$ and the box size n

$$F(n) \sim n^{\alpha}. \qquad (8)$$

A linear relationship on a double-logarithmic graph of Eq. (8) indicates that the signal presents scale-invariant or self-affine behavior. The scaling exponent α is determined by calculating the slope of the line representing the relationship between $\log F(n)$ and $\log(n)$. The Hurst exponent H can be obtained directly from the scaling exponent α; namely, $\alpha = H$ (Peng et al. 1994).

4. Results and discussion

First, to test whether SSTA in the SCS is stationary or not, an SSTA series in the central SCS (14.5°N, 112.5°E) is selected for analysis by using the well-known, robust Welch's averaged, modified periodogram method (Welch 1967) (see Fig. 3). From the log–log plot of $S(f)$ against frequency f, the power law $[S(f) \sim f^{-\beta}]$ exists obviously with spectral exponent $\beta \approx 1.39 \pm 0.177$. Because the spectral exponent β contains the information about the degree of stationary ($\beta = 0$ is white noise; $\beta < 1$, the signal is stationary; $\beta > 1$, the signal is nonstationary; and $\beta = 2$ is Brownian motion), the estimation of spectral exponent $\beta \approx 1.39$ in the data indicates that SSTA in the central SCS (14.5°N, 112.5°E) is not stationary.

In this respect, R/S analysis, DFA, and bucket-shuffling methods are employed to detect and validate the long-range dependence of SSTA in the following. The shuffling method is effective to decouple the short- from long-range correlations to infer the existence of long-range dependence by removing selected the correlations in the signals (Fitch 1983).

Figure 4 shows the results of an SSTA series in the central SCS analyzed by R/S and DFA. Both results indicate that the SSTA in the central SCS exhibits long-range dependence with an exponent value of roughly 0.98, which is larger than that of white noise ($\alpha = 0.5$) (Fig. 4). But, how solid are these results? Here, we use bucket-shuffling methods to test these results. As we expected, the exponent $\alpha \approx 0.50$ of SSTA after shuffling shows hardly any correlation (see + line in Fig. 4). That is to say, SSTA in the central SCS indeed presents long-range-dependent behavior.

As we have mentioned above, the R/S analysis has its disadvantages. For safely estimating the exponent, we will only use DFA to analysis SSTAs in the following.

Figure 5 shows the results of DFA analysis on the

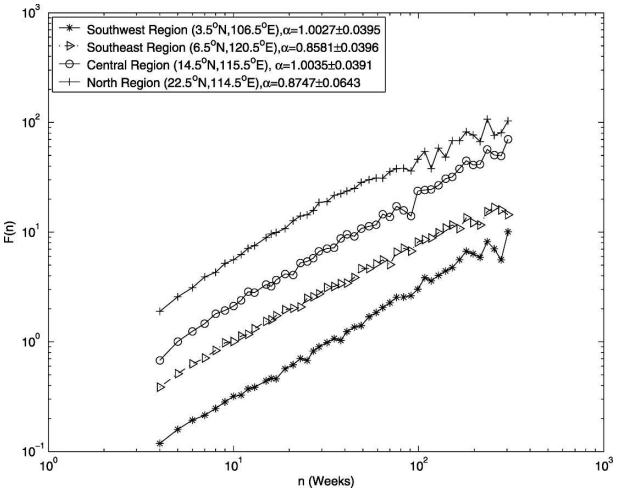

FIG. 5. The log–log plot $F(n)$ and n of the SSTA for four grid-point data ($4 \le n \le N/4$), the scaling exponents can be estimated by the least squares linear fitting of the slope. The scale of the fluctuation functions is arbitrary.

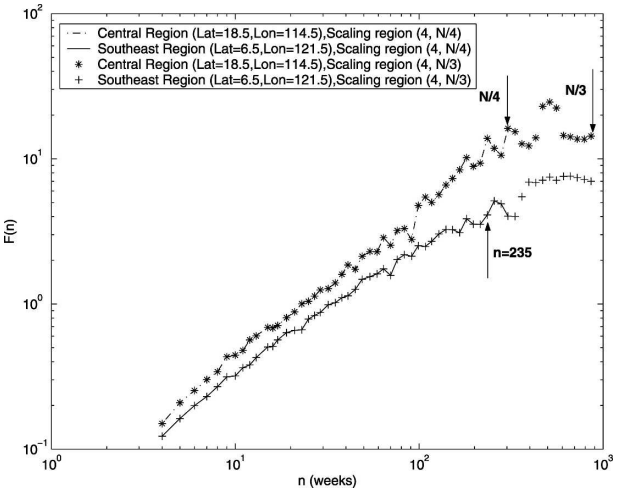

FIG. 6. The log–log plot $F(n)$ and n of the SSTA for $n_{\max} = N/4$ and $n_{\max} = N/3$, the scaling exponent's estimation is given by the slope.

data for four typical grid points, represented the southwestern (3.5°N, 106.5°E), southeastern (6.5°N, 120.5°E), northern (22.5°N, 115.5°E), and central (14.5°N, 115.5°E) regions of the SCS. Generally, the self-affine fractal of SSTA can be determined from the degree of linear fitting in a log–log plot. In simple terms, if the plotting points line up on a straight line, it means that the amount of detail at each new scale is the same and the time series is self-affine fractal. From Fig. 5, we can see that the data of four grid points in the SCS exhibit strong persistence with an exponent larger than 0.8.

For better quantification of the persistent duration of SSTAs, we extend the maximum scaling region from $N/4$ to $N/3$ (N is the total length of the series). The results show that the longer the scaling region, the more apparent the fluctuation and instability of the data becomes (Fig. 6). Note that $n = 235$ week is the time scale where the crossover of two trends occurs, which means that 4~235 weeks (roughly from 1 month to 4.5 yr) are likely to be the scaling-invariant duration of SSTAs.

From the distribution pattern of scaling exponents in the whole SCS, three features can be identified (see Fig. 7). First, all of the scaling exponents are larger than 0.8, which means that all SSTAs in SCS exhibit long-range dependence. Second, there is an increase of scaling exponents with the increase of distant from the coastline, which indicates that the key factor dominating the scaling exponent is related to the distance from the coastline. Third, because the scaling exponents in the central SCS are larger than those of the coastal region, SSTAs in the central SCS are smoother than those in the coast region.

The scaling exponents obtained from 464 grid points are plotted in the histogram (see Fig. 8). From Fig. 8, we can see that the exponents exhibit nonnormal distribution and all the α value are very large, ranging between 0.81 and 1.13. A maximum scaling exponent value of $\alpha \simeq 1.13$ occurs in the Gulf of Thailand, and a minimum value of $\alpha \simeq 0.83$ occurs near Kalimantan Island. Because these values are near the boundaries of the SCS, they are not reliable and need more careful considerations in the future.

Please note that the scaling exponent is equal to 1 ($\alpha = 1.0$); $\alpha = 1.0$ indicates that the spectral exponent $\beta = 1$ and this behavior is closely related to the classical "$1/f$" noise. Here, $1/f$ noise indicates that the dynamics of the corresponding physical system is attracted toward a critical state and the system presents self-organized criticality (Bak 1996).

5. Conclusions

In summary, we have studied the persistence of the sea surface temperature in the SCS from nonlinear time series methods such as R/S and DFA. The aim is to reveal long-term trends of the sea surface temperature change and to help to serve as a nontrivial test bed for the ocean models (Bunde et al. 2001). The results we found are as follows.

1) The scaling exponents α of SSTAs over all of the grid points in the SCS are larger than 0.8. This result reveals that pronounced long-term correlations govern the SST, and that the scaling-invariant interval may persist 4~235 weeks, roughly from 1 month to 4.5 yr.

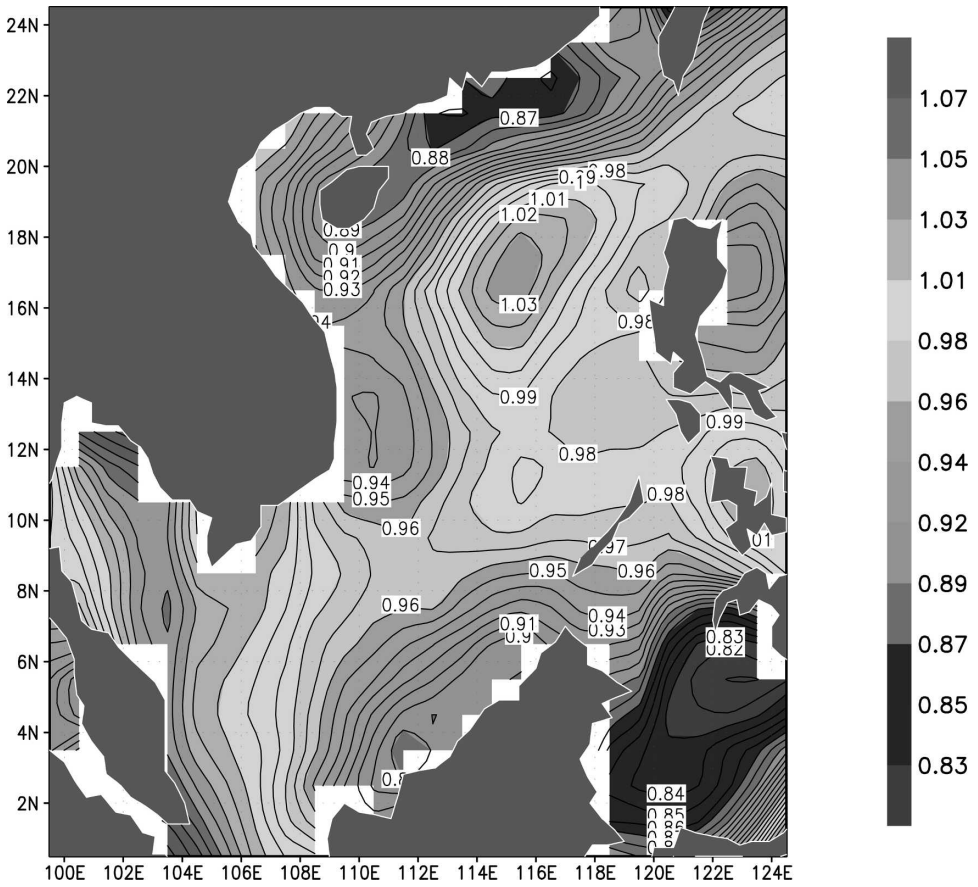

FIG. 7. The distribution of the scaling exponents for 464 gridpoint data in the SCS.

2) The "degree" of the correlations depends much on the geographic locations: near to the coastal regions the value is small, while far from the coastline the value is relative larger. This means that SSTAs in the central SCS are smoother than those of the coastal regions.
3) In the region where $\alpha = 1$, SSTA exists with an approximate $1/f$ noise behavior. This behavior is closely related to the well-known concepts of self-organized criticality, meaning that SSTAs in this area is extremely unstable and very sensitive to perturbations. Any arbitrarily small perturbation can propagate throughout the system rather than having only a local effect. The drive is a continual flow of energy or mass that arrives on a slow time scale and is dissipated on a fast time scale. All time scales are similar with power-law spectra. Although $1/f$ noise is common in nature and there are many models trying to describe it, its origin is often obscure (Sprott 2003).

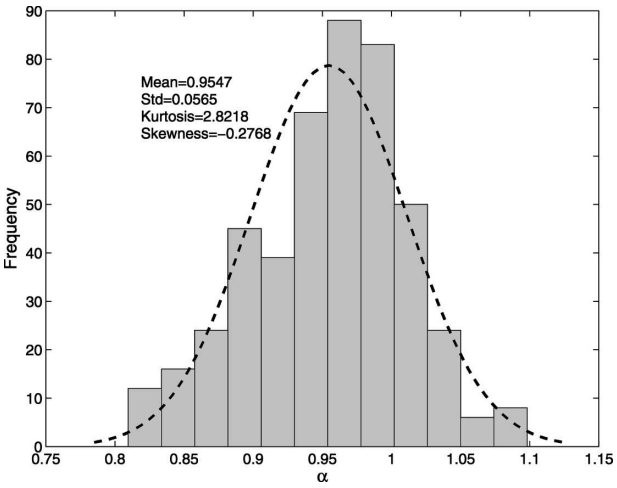

FIG. 8. The histogram of the scaling exponents for 464 gridpoint data of SSTA in SCS.

Acknowledgments. We are indebted to the Knowledge Innovation Project of the Chinese Academy of Sciences (Grant KZCX3-SW-227) and the National Natural Science foundation of China for financial support (Grants 40276004, 40306003, 40376004), and thanks are also given to the National Center for Atmospheric Research (NCAR) for providing the data.

REFERENCES

Bak, P., 1996: *How Nature Works: The Science of Self-Organized Criticality.* Springer-Verlag, 212 pp.

Bunde, A., S. Havlin, B. E. Koscielny, and H. J. Schellnhuber, 2001: Long term persistence in the atmosphere: Global laws and tests of climate models. *Physica A,* **302,** 255–267.

Chu, P. C., C. P. Chang, and Y. Chen, 1997: Temporal and spatial variabilities of the South China Sea surface temperature anomaly. *J. Geophys. Res.,* **102,** 20 937–20 955.

Feder, J., 1988: *Fractals.* Plenum Press, 310 pp.

Fitch, W. M., 1983: Random sequences. *J. Mol. Biol.,* **163,** 171–176.

Havlin, S., S. V. Buldyrev, A. Bunde, A. L. Goldberger, P. C. Ivanov, C. K. Peng, and H. E. Stanley, 1999: Scaling in nature: From DNA through heartbeats to weather. *Physica A,* **273,** 46–69.

Hurst, H. E., 1951: Long term storage of reservoirs: An experimental study. *Trans. Amer. Soc. Civ. Eng.,* **116,** 770–799.

Kiraly, A., and I. Janosi, 2002: Stochastic modeling of daily temperature fluctuations. *Phys. Rev. E,* **65,** doi:10.1103/PhysRevE.65.051102.

Liu, Y. H., P. Cizeau, M. Meyer, C. K. Peng, and H. E. Stanley, 1997: Correlations in economic time series. *Physica A,* **245,** 437–440.

Matsoukas, C., S. Islam, and I. Rodriguez-Iturbe, 2000: Detrended fluctuation analysis of rainfall and streamflow time series. *J. Geophys. Res.,* **105,** 29 165–29 172.

North, C. P., and D. I. Halliwell, 1994: Bias in estimating fractal dimension with the rescaled-range (R/S) technique. *Math. Geol.,* **26,** 531–555.

Ose, T., Y. Song, and A. Kitoh, 1997: Sea surface temperature in the South China Sea: An index for the Asian monsoon and ENSO system. *J. Meteor. Soc. Japan,* **75,** 1091–1107.

Peng, C. K., S. V. Buldyrev, S. Havlin, M. Simons, H. E. Stanley, and A. L. Goldberger, 1994: Mosaic organization of DNA nucleotides. *Phys. Rev. E,* **49,** 1685–1689.

——, S. Havlin, J. M. Hausdorff, J. E. Mietus, H. E. Stanley, and A. L. Goldberger, 1995: Fractal mechanisms and heart rate dynamics—Long-range correlations and their breakdown with disease. *J. Electrocardiol.,* **28,** 59–65.

Peters, O., C. Hertlein, and K. Christensen, 2002: A complexity view of rainfall. *Phys. Rev. Lett.,* **88,** doi:10.1103/PhysRevLett.88.018701.

Qu, T., 2001: The role of ocean dynamics in determining the mean seasonal cycle of the South China Sea surface temperature. *J. Geophys. Res.,* **106,** 6943–6955.

Reynolds, R. W., and T. M. Smith, 1994: Improved global sea surface temperature analyses using optimum interpolation. *J. Climate,* **7,** 929–948.

Sprott, J. C., 2003: *Chaos and Time-Series Analysis.* Oxford University Press, 528 pp.

Tian, J. W., J. S. Xu, and E. B. Wei, 2000: The wavelet analysis of satellite sea surface temperature in the South China Sea and the Pacific Ocean. *Chin. Sci. Bull.,* **45,** 2187–2192.

Wang, D. X., F. X. Zhou, G. Fu, and Z. H. Qin, 1996: Numerical study on the interannual osillation of sea surface temperature in the South China Sea. *Chin. J. Oceanol. Limnol.,* **14,** 61–67.

Welch, P. D., 1967: The use of fast Fourier transform for the estimation of power spectra: A method based on time averaging over short, modified periodograms. *IEEE Trans. Audio Electroacoust.,* **AU-15,** 70–73.